Charge-ordering and magnetic phase transitions in θ-(BDT-TTP)$_2$Cu(NCS)$_2$

K. Yakushi, K. Yamamoto, M. Simonyan, J. Ouyang, and C. Nakano
Institute for Molecular Science, Myodaiji, Okazaki, 444-8585, Japan

Y. Misaki and K. Tanaka
Department of Molecular Engineering, Kyoto University, Kyoto, 606-8501, Japan

(Received 24 May 2002; revised manuscript received 9 August 2002; published 5 December 2002)

We present the polarized Raman spectra and magnetic susceptibility of θ-(BDT-TTP)$_2$Cu(NCS)$_2$ which undergoes a charge-ordering phase transition at $T_{CO}\sim 250$ K. From the splitting of the ν_2 band, the charge-disproportionation ratio δ is estimated as 0.4 at ~ 10 K. The linewidth of ν_2 suggests the fluctuation in charge distribution above T_{CO}. The magnetic susceptibility of $30\ \mathrm{K} < T < 300$ K follows the Curie–Weiss Law with the Curie constant of 0.154 emuK/mol and Weiss temperature of -29 K. The single-crystal ESR experiment shows a magnetic phase transition to a spin-singlet state at 5 K. The polarized Raman spectra and magnetic property suggest the view that the positive charge is vertically ordered along the *b*-axis.

DOI: 10.1103/PhysRevB.66.235102 PACS number(s): 71.30.+h, 78.30.Jw, 78.20.Ci

The charge ordering (CO) in organic charge-transfer (CT) salts draws much attention, since the theoretical studies suggest the relation between the charge fluctuation and the pairing mechanism in superconductivity (SC).[1,2] The CT salts with the nondimerized structure are distinguished from the strongly dimerized κ-type BEDT-TTF [BEDT-TTF $=bis$(ethylenedithiolo)tetrathiafulvalene is hereafter abbreviated as ET] salts, in which the theoretical calculation suggests that the antiferromagnetic spin fluctuation mediates SC.[3] Some nondimerized organic CT salts are theoretically considered as the candidates for this unconventional SC (see the compounds shown in Table I of Ref. 2). The experimental study on charge ordering of organic CT salts has been conducted most intensively in θ-type ET salts.[4,5,6] The θ-ET salt is a quarter-filled quasi-two-dimensional (Q2D) system without a dimerized ET unit. In nondimerized θ-ET salts, the charge localization is accompanied by charge disproportionation (CD) and generates charge-rich and charge-poor sites such as $(0.5+\delta, 0.5-\delta)$. The CD lowers the symmetry of the unit cell, and forms a new periodic lattice with nonuniform charge distribution. Such CO phase transitions have been discovered in nondimerized quarter-filled Q1D system, (DI-DCNQI)$_2$Ag,[7] nondimerized Q2D system, θ-(ET)$_2$RbZn(SCN)$_4$,[8,9] and θ-(BDT-TTP)$_2$Cu(NCS)$_2$,[10] and weakly dimerized Q2D system, α-(ET)$_2$I$_3$.[11] Recently, the CO phase transition was found in (TMTTF)$_2$X (Refs. 12, 13, and 14) (X=PF$_6$, AsF$_6$, SbF$_6$), which is a more strongly dimerized Q1D quarter-filled organic CT salt. The localization of charge is widely found in organic CT salts, and CO seems to be associated with the various metal–insulator and insulator–insulator phase transitions,[15] although the CO state is confirmed only in a few compounds described above.

The CO pattern in a variety of ET-based CT salts was theoretically considered in the framework of mean-field theory.[16,17] Seo examined the three types of CO patterns, the horizontal, diagonal, and vertical stripes,[17] the stability of which depends upon the transfer integrals *t*, intersite Coulomb energy *V*, and on-site Coulomb energy *U*, and therefore upon the arrangement of molecules. The stability of each CO pattern in θ-type crystal is theoretically considered by McKenzie *et al.*[18] and Clay *et al.*[19] as well. Based on the Raman spectra, Ouyang *et al.* reported a CO phase transition at $T_{CO}\sim 250$ K in θ-(BDT-TTP)$_2$Cu(NCS)$_2$ [BDT-TTP $=2,5$-*bis*(1, 3-dithiol-2-ylidene)-1, 3,4,6-tetrathia-pentalene] and suggested the vertical stripe for the CO pattern.[10] However, they have not studied the magnetic property that gives some information about the CO pattern. In this report, we first present the parameter δ, and discuss the charge fluctuation above T_{CO} and structural fluctuations below T_{CO}. Second, we evaluate the magnitude of the magnetic interaction between the localized charges, and present the finding of a magnetic phase transition in this compound. Third, we discuss the CO pattern based on the magnetic property and the selection rule in the polarized Raman spectra.

The single crystals of θ-(BDT-TTP)$_2$Cu(NCS)$_2$ were prepared by an electrochemical method.[20] The θ-type crystal was selected by means of a reflectivity measurement.[21] The crystal shape is a thin plate elongated along the *b*-axis to develop a (100) crystal face. The crystal face and the crystallographic axes were determined by the x-ray diffraction method. The Raman spectrum was measured on a Renishaw Ramascope System-1000 with backscattering geometry. The cryostat system for this spectrometer is described elsewhere.[22] The scattered light was analyzed using a polarization filter with an extinction ratio of 10^{-4}. For example, the (*c*,*b*) spectrum denotes an experimental condition in which the laser is polarized along the *c*-axis, and the analyzer is polarized along the *b*-axis, with the wave vector being parallel to the a^*-axis owing to the back-scattering geometry. We used a He–Ne laser with wavelengths at 632.8 nm. The laser was irradiated at the spot area with 20 μm diam on the crystal face. The intensity was reduced to less than 50–100 μW to avoid the heating effect.[23] The details of our consideration of the heating effect were described elsewhere.[24] The static magnetic susceptibility was measured on a SQUID magnetometer (Quantum Design MPMS 7000) by applying a magnetic field of 1 T. About 1 mg of single crystals was aligned with silicone grease on a quartz plate. A magnetic field was applied along the *b*- and *c*-axes, and no anisotropy was observed between these two axes. ESR mea-

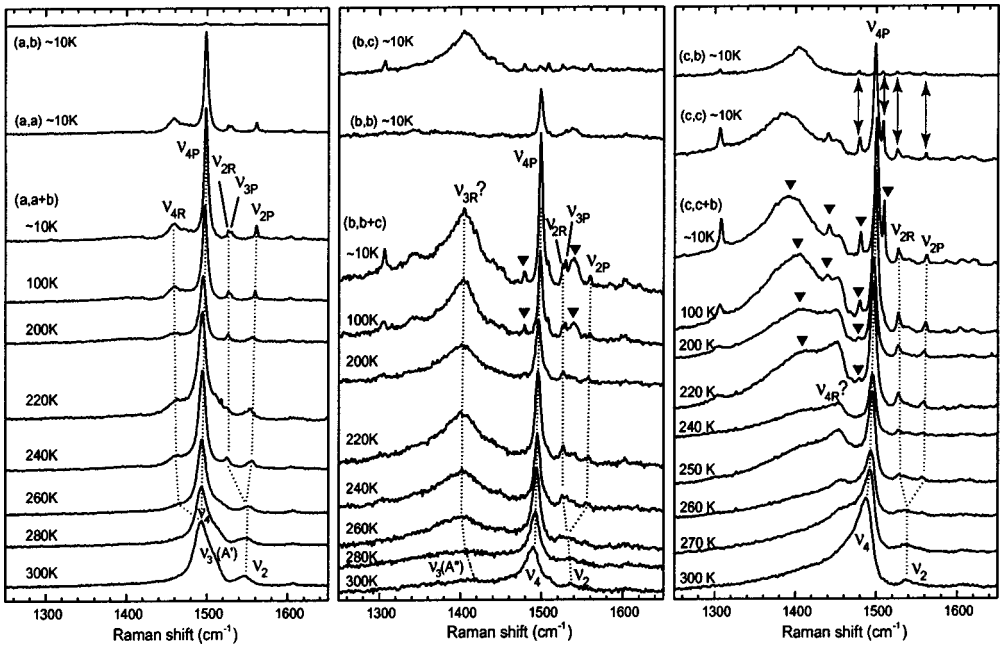

FIG. 1. Polarized Raman spectra measured on the (100) and (001) crystal faces. ν_{jP} and ν_{jR} denote the ν_j mode at the charge-poor and charge-rich sites, respectively. The arrows in 1(c) show that the selection rule required by the glide-plane symmetry is broken. The triangles show additional bands that suggest the doubling of the unit cell.

surements were carried out on an ESR spectrometer with an *X*-band cavity (Bruker ESP-300E) using a single crystal mounted on a quartz rod. The temperature was controlled within ± 0.1 K using a helium-gas flow-type cryostat (Oxford ESR-900 and ITC-4).

BDT-TTP has five C═C bonds [see the structural formula shown in Fig. 2(a)]. The five C═C stretching modes of BDT-TTP are classified into two infrared-active and three Raman-active modes, if we assume D_{2h} symmetry. According to the normal coordinate analysis of the BDT-TTP molecule, these Raman active modes ν_2, ν_3, and ν_4, are located at around 1500 cm^{-1} and are separated from other fundamental modes.[25] The C═C stretchings are significantly mixed in BDT-TTP^0, whereas they are rather separated from each other in BDT-TTP$^+$. Thus ν_2 and ν_3 in BDT-TTP$^+$ are assigned mainly to the in-phase C═C stretching modes of outer-rings and bridges, respectively, and ν_4 is assigned to the C═C stretching mode of the inner-ring. Taniguchi *et al.* reported the *ab initio* calculation for the EMV coupling constants of all a_g modes in BDT-TTP$^+$.[26] According to their calculation, the coupling constant of ν_3 is the strongest among the 11 a_g modes, and those of ν_2 and ν_4 are significantly small. This quantum-chemical calculation is supported by the optical conductivity of this compound. No vibronic modes corresponding to ν_2 and ν_4 is observed, as shown in Table I. The crystal of θ-$(BDT\text{-}TTP)_2Cu(NCS)_2$ belongs to a monoclinic system with space group of *Cc*.[27] The arrangement of molecules quite resembles that of θ-$(ET)_2TlZn(SCN)_4$.[28] The unit cell involves two conducting layers separated by the anion layer. The donor molecules in the conducting layer take a herringbone structure with a dihedral angle of 128° (see Fig. 1 of Ref. 29). The two molecules in the periodic unit in the conducting layer are connected by glide-plane symmetry. Since the factor group of this crystal is C_s, the $\mathbf{q}=0$ crystal mode is classified into A' (in-phase) and A'' (out-of-phase) modes.

The polarized Raman spectra measured on the (100) and (001) crystal faces are shown in Fig. 1, and the peak frequencies at three temperatures are listed in Table I along with the infrared-active bands. The 300 K spectra show two broad bands in $(c,c+b)$, three broad bands including a very weak one at ~ 1420 cm^{-1} in $(b,b+c)$, and three broad bands including a shoulder at ~ 1510 cm^{-1} in $(a,a+b)$. Considering the room-temperature frequency data of $\nu_2(0)=1555$ cm^{-1}, $\nu_3(0)=1525$ cm^{-1}, $\nu_4(0)=1504$ cm^{-1}, $\nu_2(0.5+)=1533$ cm^{-1}, $\nu_3(0.5+)=1500$ cm^{-1}, and $\nu_4(0.5+)=1480$ cm^{-1},[10] we assigned three groups to ν_2, ν_3, and ν_4 as shown in Fig. 1, where the value in parenthesis is the average charge on BDT-TTP. The very broad band at ~ 1420 cm^{-1} may be assigned to the factor group component (A'' symmetry) of ν_3, because this band exclusively appears in the (b,c) and (c,b) polarizations and the EMV coupling constant of ν_3 is strongest. Below the CO phase transition temperature ($T_{CO}\sim 250$ K), for example at 240 K, the number of Raman-active bands increases to 5. As shown in Fig. 1, ν_2 at 240 K shows a splitting in all of the spectra. Since the EMV coupling constant of ν_2 is small, we can safely assign these split bands to ν_{2P} in a charge-poor site and to ν_{2R} in a charge-rich site. The strongest band at 1494 cm^{-1} is assigned to ν_{4P} based on the intensity and frequency of $\nu_4(0)$ (see Ref. 10 for the intensity). Since the EMV coupling constant of ν_3 is calculated to be very large, the strong and broad band at ~ 1403 cm^{-1} in the $(b,b+c)$ spectrum may be assigned to ν_{3R}. The remaining broad band at ~ 1460 cm^{-1} in the $(a,a+b)$ spectrum is ascribed to ν_{4R}. The ν_{3P} band is

TABLE I. Raman and infrared bands associated with the C═C stretching mode.

Raman bands						IR bands					
300 K		240 K		~10 K		300 K		240 K		15 K	
1537,[b] 1538,[c] 1546[a]	ν_2	1554,[a] 1557[c]	ν_{2P}	1561[a,b,c]	ν_{2P}						
				1540[b]	⋯						
~1510[a]	$\nu_3(A')$			1530[a,b]	ν_{3P}						
		1524,[a] 1528[c]	ν_{2R}	1527[a,b,c]	ν_{2R}						
				1507,[b] 1509[c]	⋯						
1487,[c] 1491,[b] 1492[c]	ν_4	1494,[a,b] 1495[c]	ν_{4P}	1498,[a] 1499,[b] 1500[c]	ν_{4P}						
				1479,[b] 1480[c]	⋯						
		~1460,[a]	ν_{4R}	~1456,[c] 1459[a]	ν_{4R}						
		~1453[c]	ν_{4R}?								
				1442[c]	⋯						
~1420[b]	$\nu_3(A'')$	~1403[b]	ν_{3R}?	1404[b,c]	ν_{3R}?	~1480[d,e] (very broad dip)	ν_3?	1394[d] (strong)	ν_{22}	1398[d] (strong)	ν_{22}
				~1391[c]	⋯						

Polarizations are denoted by a for $(a,a+b)$, b for $(b,b+c)$, and c for $(c,c+b)$ in the Raman spectra, and by d for $E\|c$, and e for $E\|b$ in the IR spectra of Ref. 10.

missing at 240 K, which appears at 1530 cm^{-1} more clearly in the $(b,b+c)$ and $(a,a+b)$ spectra taken at ~10 K.[30] Below 220 K, many additional bands appear; they are denoted by triangles. The appearance of these additional bands suggests a doubling of the unit cell. Since the doubled unit cell involves four BDT-TTP molecules, the maximum number of Raman-active C═C stretching modes is twelve at the most.[31] We consider that the additional broad bands at 1540 cm^{-1} and 1391 cm^{-1} are EMV coupled, because these bands disappear in the $(a,a+b)$ polarization, the direction of which is perpendicular to the conducting plane. It is difficult to perform the complete assignment without the aid of isotope-substituted compounds. The unambiguous assignment in a whole temperature range is given to the bands at 1561 cm^{-1} and 1527 cm^{-1}, which is assigned to ν_{2P} and ν_{2R}, respectively. The temperature dependence of ν_2 and ν_4 is drawn in Fig. 2(b), along with electrical resistivity and magnetic susceptibility, which will be discussed below. As shown in Fig. 2(b), all of these bands show splitting (ν_{jP} and ν_{jR}) near T_{CO}. The splitting between ν_{2P} and ν_{2R} at each temperature is associated with the order parameter of this phase transition. Assuming a linear relationship between the frequency and charge on the molecule, we roughly estimate the deviation of charge δ from 0.5 in the CD state $(BDT\text{-}TTP)^{0.5+\delta}(BDT\text{-}TTP)^{0.5-\delta}$ using the equation $\delta=(\nu_{2P}-\nu_{2R})/[4\{\nu_2(0)-\nu_2(0.5)\}]$. The δ value at ~10 K is ~0.4. We applied this relation to the tentatively assigned ν_{4P} and ν_{4R} as well and obtained the same value.

The ν_2 band shows a clear splitting with a separation of $\delta\omega=34\ cm^{-1}$ at 250 K in the $(c,c+b)$ spectrum, and these two peaks, which correspond to charge-poor (ν_{2P}) and charge-rich (ν_{2R}) sites, merge into a broad single band above 260 K. Very similar behavior is found in the $(b,b+c)$ spectrum and is more clearly seen in the $(a,a+b)$ spectrum. The splitting of the ν_2 band means that the charge is localized on the time scale of $1/\delta\omega\sim1$ ps, inducing CD with $\delta=0.3_5$. The coalescence of the split bands above T_{CO} means that the high-temperature phase forms a uniform charge distribution with $\delta=0$. The linewidth (~18 cm^{-1}) at room temperature is significantly broader than that (~8 cm^{-1}) of the corresponding band in metallic $(BDT\text{-}TTP)_2SbF_6$,[10] which has a uniform charge distribution. This broad linewidth is ascribed to the fluctuation of charge, the rate of which is slower than $\delta\omega$. If the charge is fluctuating slowly around $\delta=0$, the line shape of the broad band is roughly given by the equation, $\{(r+1)(\delta\nu)^2/2+(r-1)\Delta\nu\delta\nu\}/[\{(\Delta\nu)^2-(\delta\nu/2)^2\}^2/\nu_f^2+(2\Delta\nu)^2]$, where $\Delta\nu=\nu-\nu_0$, $\nu_0=(\nu_P+\nu_R)/2$, $\delta\nu=\nu_P-\nu_R$, r is the intensity ratio I_P/I_R, and ν_f is the rate of fluctuation between P and R sites.[32] Applying this equation to ν_2 in $(c,c+b)$ and $(a,a+b)$ so as to reproduce the linewidth, we obtained ν_f as 20 and 19 cm^{-1}, respectively, which are almost the same with each other. The position of ν_2 in the $(a,a+b)$ spectrum is slightly higher than that in the $(c,c+b)$ and $(b,b+c)$ spectra (see Table I). This simple model cannot quantitatively explain the peak shift from $(\nu_P+\nu_R)/2$. As shown in Fig. 2(a), this compound is nonmetallic above T_{CO} as well as below T_{CO}. Therefore, the relatively high conductivity ($\rho_{RT}\sim10^{-2}\ \Omega$ cm) can be ascribed to the thermally activated incoherent hopping of charges that causes the fluctuation in the charge distribution.

As shown in Fig. 2(c), the magnetic susceptibility shows no anomaly at T_{CO}, a behavior that is commonly observed in θ-$(ET)_2RbZn(SCN)_4$.[4] The susceptibility above 30 K nearly follows the Curie–Weiss Law with the Curie constant of 0.154 emu K/mol and a Weiss temperature of −29 K. The magnetic moment per $(BDT\text{-}TTF)_2Cu(NCS)_2$ is reduced to 64% of that corresponding to a free spin. The susceptibility levels off below 30 K and shows an extrinsic increase below 3 K. By contrast, the ESR intensity shows a maximum at ~10 K and abruptly drops at 5 K without changing the line shape [see the inset of Fig. 2(c)]. This result indicates that θ-$(BDT\text{-}TTP)_2Cu(NCS)_2$ undergoes a magnetic phase transition at $T_M=5$ K and goes into a spin singlet state. The

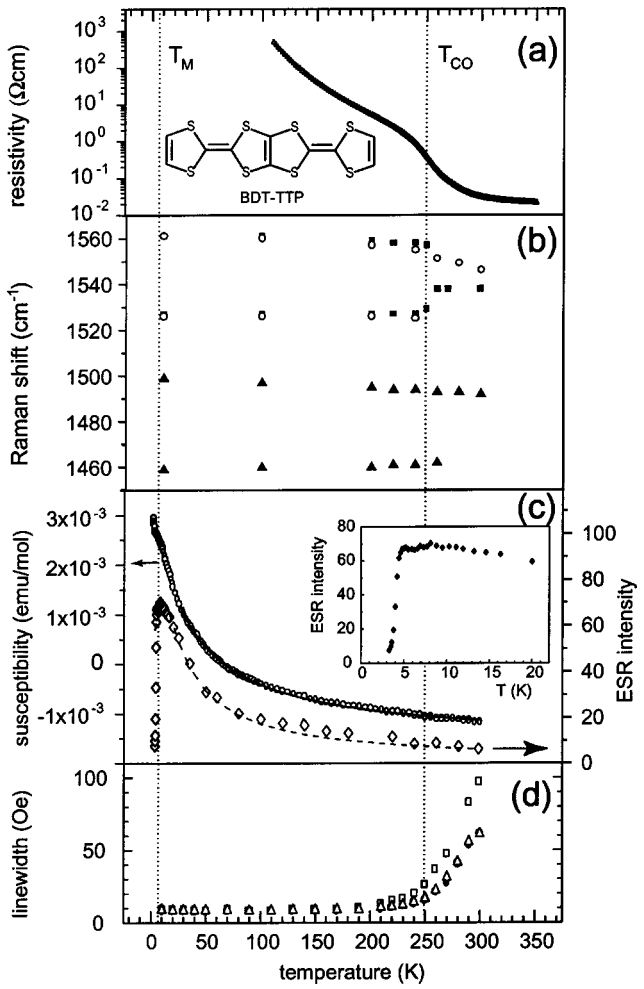

FIG. 2. (a) Temperature dependence of resistivity. (b) Temperature dependence of the frequency of ν_2 (solid square) in the $(c,c+b)$ spectrum, ν_2 (open circle) in $(a,a+b)$, and ν_4 (solid triangle) in $(a,a+b)$. (c) Magnetic susceptibility and ESR intensity. The solid and broken lines are respectively the best-fit curves of the Curie–Weiss model and the Bonner–Fisher model with $J=-7.9$ K. The low-temperature region of the ESR intensity is expanded in the inset. (d) ESR linewidth. Open squares, open triangles, and solid circles, respectively, correspond to the signals of $H\|a^*$, $H\|c$; and $H\|b$. T_{CO} and T_M represent the charge-ordering and magnetic phase transition temperatures, respectively.

two-step phase transition in this compound resembles the case of θ-$(ET)_2RbZn(SCN)_4$, which gives $T_{CO}=200$ K and $T_M=40$ K.[4] As shown in Fig. 2(c), the ESR intensity above 5 K is well fitted to the 1D Heisenberg model with $J=-7.9$ K.[33] The absolute value is much smaller than the corresponding value $(J=-157$ K) of θ-$(ET)_2RbZn(SCN)_4$.[4] As shown in Fig. 2(d), the linewidth steeply decreases from 300 K and levels off at 200 K. Similar behavior is reported at the metal–insulator transition temperatures of θ-$(ET)_2CsM(SCN)_4$ (M=Co and Zn) (Ref. 34) and θ-$(ET)_2Cu_2(CN)[N(CN)_2]$.[5] A sharp drop in linewidth is reported at the first-order phase transition of θ-$(ET)_2RbM(SCN)_4$ (M=Co and Zn) (Ref. 34) and α-$(ET)_2I_3$.[35,36] Since the decrease of ESR linewidth is commonly found in the θ-type ET salts, the spin relaxation mechanism seems to be strongly correlated with the CO phase transition.

Ouyang *et al.* suggested that the charge-rich (hole) sites were aligned along the stacking *b*-axis (vertical stripe) by comparing the spectral shape of the optical conductivity in the infrared region with the theoretical spectrum calculated by Tajima *et al.*[10,37] If the holes are aligned vertically, the exchange interaction between the magnetic moments of the adjacent holes is expected to be very weak according to Seo's theoretical study.[17] Therefore, the small exchange energy ($|J|\sim 8$ K) of this compound strongly supports the vertical stripe for the CO pattern. If the holes are aligned vertically, the two sites in the periodic unit in the conducting layer becomes nonequivalent with each other, in other words, the glide-plane symmetry cannot be preserved below T_{CO}. As shown by the arrows in the (c,b) and (c,c) spectra at $\sim$10 K, the selection rule required by glide-plane symmetry is clearly broken. As we described above, several additional bands, which suggest the doubling of the unit cell, appear at this temperature. If the doubling of the unit cell occurs along the *b*-axis and is long-range ordered at $\sim$10 K, the magnetic moments of the holes are alternatively linked along the *b*-axis.[38] This structure is incompatible with the spin-Peierls-type magnetic phase transition at 5 K. We therefore speculate that the structure is short-range ordered and still fluctuating at $\sim$10 K. At 200 K, all additional bands disappear with the exception of the weak bands at 1480 cm^{-1} and $\sim$1400 cm^{-1} as shown in the $(c,c+b)$ spectrum. We suppose that the structural fluctuation exists very weakly but the unit cell is essentially undoubled at 200 K.[39] We examined the selection rule in the polarized Raman spectrum at 200 K and confirmed that the glide-plane symmetry was already broken at 200 K. As shown in Table I, there observed a broad dip with a width of $\sim$200 cm^{-1} in the infrared spectrum at 300 K (see Fig. 2 of Ref. 10). If this very broad dip is attributed to the ν_3 mode induced by the EMV interaction,[40] this dip should appear only in the $E\|b$ spectrum, because the EMV interaction works only in the out-of-phase mode (A'' symmetry). However, the dip in $E\|c$ is stronger than that in $E\|b$. This means that the glide-plane symmetry is already broken at room temperature, although ν_2 appears as a single band and x-ray diffraction experiment indicates the existence of the glide plane at room temperature. These contradictory results seem to be ascribed to the fluctuation rate. As we discussed before, the fluctuation rate is $\sim$20 cm^{-1}, which is much smaller than the frequencies of ν_2. This seems to be the reason for the breaking of the selection rule in the infrared spectrum. Summarizing above, all the results suggests that the CO pattern in this compound is the vertical stripe along the *b*-axis, which is different from the horizontal stripe in θ-$(ET)_2RbZn(SCN)_4$.[9] Clay *et al.* calculated the stabilization energy of three CO patterns in θ-type CT salts, and showed that the horizontal or diagonal stripe was more stable than the vertical stripe in a realistic range of V.[19] On the other hand, McKenzie *et al.* predicted a vertical stripe for the CO pattern of the θ-type CT salts.[18] θ-$(BDT\text{-}TTP)_2Cu(NCS)_2$ seems to be understood in the framework of the latter theory.

In conclusion, the electronic phase of θ-(BDT-TTP)$_2$Cu(NCS)$_2$ is characterized as follows. Above $T_{CO} \sim 250$ K, this compound is an antiferromagnetically interacting insulator with a dynamic charge fluctuation and relatively high conductivity. Below T_{CO}, the charge is localized and forms a vertical stripe, which leads to an increase of the charge gap. Structural fluctuation of unit-cell doubling begins at ~200 K and continuously grows down to ~10 K. At $T_M = 5$ K, the compound undergoes magnetic phase transition and forms a spin singlet state.

This research was supported by a Grant-in-Aid for Scientific Research (No. 13440214) from the Ministry of Education, Culture, Sports, Science, and Technology of Japan.

[1] S. Mazumdar, R. T. Clay, and D. K. Campbell, Phys. Rev. B **62**, 13400 (2000).
[2] J. Merio and R. H. McKenzie, Phys. Rev. Lett. **87**, 237002 (2001).
[3] J. Schmalian, Phys. Rev. Lett. **81**, 4232 (1998); H. Kondo and T. Moriya, J. Phys. Soc. Jpn. **67**, 3695 (1998); H. Kino and K. Kotani, *ibid.* **67**, 3691 (1998).
[4] H. Mori, S. Tanaka, and T. Mori, Phys. Rev. B **57**, 12 023 (1998).
[5] T. Komatsu, H. Sato, T. Nakamura, N. Mtsukawa, H. Yamochi, G. Saito, M. Kusunoki, K. Sakaguchi, and S. Kagoshima, Bull. Chem. Soc. Jpn. **68**, 2233 (1995).
[6] M. Watanabe, Y. Nogami, K. Oshima, H. Mori, and S. Tanaka, J. Phys. Soc. Jpn. **68**, 2654 (1999).
[7] K. Hiraki and K. Kanoda, Phys. Rev. Lett. **80**, 4737 (1998).
[8] K. Miyagawa, A. Kawamoto, and K. Kanoda, Phys. Rev. B **62**, R7679 (2000).
[9] K. Yamamoto, K. Yakushi, K. Miyagawa, K. Kanoda, and A. Kawamoto, Phys. Rev. B **65**, 085110 (2002).
[10] J. Ouyang, K. Yakushi, Y. Misaki, and K. Tanaka, Phys. Rev. B **63**, 054301 (2001).
[11] Y. Takano, K. Hiraki, H. M. Yamamoto, T. Nakamura, and T. Takahashi, Synth. Met. **120**, 1081 (2001).
[12] D. S. Chow, F. Zamborszky, A. Alavi, D. J. Tantillo, A. Bauer, C. A. Merlic, and S. E. Brown, Phys. Rev. Lett. **85**, 1698 (2000).
[13] F. Nad, P. Monceau, C. Carcel, and J. M. Fabre, Phys. Rev. B **62**, 1753 (2000).
[14] P. Monceau, F. Ya, and S. Brazovskii, Phys. Rev. Lett. **86**, 4080 (2001).
[15] For example, K. Carneiro, J. C. Scott, and E. M. Engler, Solid State Commun. **50**, 477 (1984); M. Tokumoto, H. Anzai, T. Ishiguro, G. Saito, H. Kobayashi, R. Kato, and A. Kobayashi, Synth. Met. **19**, 215 (1987).
[16] H. Kino and H. Fukuyama, J. Phys. Soc. Jpn. **65**, 2158 (1996).
[17] H. Seo, J. Phys. Soc. Jpn. **69**, 805 (2000).
[18] R. H. McKenzie, J. Merino, J. B. Marston, and D. P. Sushkov, Phys. Rev. B **64**, 085109 (2001).
[19] R. T. Clay, S. Mazumdar, and D. K. Campbell, J. Phys. Soc. Jpn. **71**, 1816 (2002).
[20] Y. Misaki, T. Kochi, M. Taniguchi, H. Fujiwara, T. Matsui, T. Yamabe, K. Tanaka, T. Mori, T. Kawamoto, M. Aragaki, H. Mori, and S. Tanaka (private communication).
[21] The crystals involve two modifications. The θ-type crystal exhibits the strong and sharp phonon bands at 648 and 2116 cm^{-1}.
[22] J. Ouyang, J. Dong, K. Yakushi, K. Takimiya, and T. Otsubo, J. Phys. Soc. Jpn. **68**, 3708 (1999).
[23] This crystal was photo-damaged, when the laser power in the same area is higher than 1 mW.
[24] M. Maksimuk, K. Yakushi, H. Taniguchi, K. Kanoda, and A. Kawamoto, J. Phys. Soc. Jpn. **70**, 3728 (2001).
[25] J. Ouyang, K. Yakushi, T. Kinoshita, N. Nanbu, M. Aoyagi, Y. Misaki, and K. Tanaka, Spectrochim. Acta, Part A **58**, 1643 (2002).
[26] M. Taniguchi, Y. Misaki, and K. Tanaka, Solid State Commun. **114**, 75 (2000).
[27] The lattice constants are $a = 37.176(6)$, $b = 4.001$, $c = 10.957(5)$ Å, and $\beta = 102.40(3)°$, with $Z = 2$.
[28] H. Mori, S. Tanaka, T. Mori, A. Kobayashi, and H. Kobayashi, Bull. Chem. Soc. Jpn. **71**, 797 (1998).
[29] K. Yakushi, K. Yamamoto, J. Ouyang, M. Simonyan, C. Nakano, Y. Misaki, and K. Tanaka, in Proceedings of the ISCOM2001, Synth. Met. (to be published).
[30] The 1530 cm^{-1} band nearly overlaps ν_{2R} at 1527 cm^{-1}. The former band is enhanced by the Ar$^+$ laser, which also enhances the other vibrational modes of the charge-poor molecule (Ref. 10).
[31] Strictly speaking, the unit cell contains eight molecules because it contains two conducting layers separated by an anion layer. Since the interlayer interaction seems to be weak, we consider every mode within the same conduction layer as doubly degenerate.
[32] H. S. Gutowsky and A. Saika, J. Chem. Phys. **21**, 1688 (1953).
[33] J. C. Bonner and M. E. Fischer, Phys. Rev. A **135**, A640 (1964).
[34] H. Mori, S. Tanaka, and T. Mori, J. Phys. I **6**, 1987 (1996).
[35] T. Sugano, G. Saito, and M. Kinoshita, Phys. Rev. B **34**, 117 (1986).
[36] B. Rothaemel, L. Forro, J. R. Cooper, J. S. Schiling, M. Wegner, P. Bele, H. Brunner, D. Schweitzer, and H. J. Keller, Phys. Rev. B **34**, 704 (1986).
[37] H. Tajima, S. Kyoden, H. Mori, and S. Tanaka, Phys. Rev. B **62**, 9378 (2000).
[38] If the doubling occurs along the *c*-axis, the system is regarded as a spin ladder, which also has a spin gap.
[39] This speculation is consistent with the result of the x-ray diffraction; no diffraction spot or diffuse streak corresponding to a superlattice was found in the imaging plate of the x-ray diffractometer at 100 K.
[40] The similar dip is observed at ~1435 cm^{-1} in metallic (BDT-TTP)$_2$SbF$_6$: J. Ouyang, K. Yakushi, Y. Misaki, and K. Tanaka, J. Phys. Soc. Jpn. **67**, 3191 (1998).